NASA/TM—2013-216562 AIAA–2013–3727

Investigation of Insulation Materials for Future Radioisotope Power Systems

Peggy A. Cornell, Frances I. Hurwitz, and David L. Ellis
Glenn Research Center, Cleveland, Ohio

Paul C. Schmitz
Vantage Partners, LLC, Brook Park, Ohio

December 2013

NASA STI Program . . . in Profile

Since its founding, NASA has been dedicated to the advancement of aeronautics and space science. The NASA Scientific and Technical Information (STI) program plays a key part in helping NASA maintain this important role.

The NASA STI Program operates under the auspices of the Agency Chief Information Officer. It collects, organizes, provides for archiving, and disseminates NASA's STI. The NASA STI program provides access to the NASA Aeronautics and Space Database and its public interface, the NASA Technical Reports Server, thus providing one of the largest collections of aeronautical and space science STI in the world. Results are published in both non-NASA channels and by NASA in the NASA STI Report Series, which includes the following report types:

- TECHNICAL PUBLICATION. Reports of completed research or a major significant phase of research that present the results of NASA programs and include extensive data or theoretical analysis. Includes compilations of significant scientific and technical data and information deemed to be of continuing reference value. NASA counterpart of peer-reviewed formal professional papers but has less stringent limitations on manuscript length and extent of graphic presentations.

- TECHNICAL MEMORANDUM. Scientific and technical findings that are preliminary or of specialized interest, e.g., quick release reports, working papers, and bibliographies that contain minimal annotation. Does not contain extensive analysis.

- CONTRACTOR REPORT. Scientific and technical findings by NASA-sponsored contractors and grantees.

- CONFERENCE PUBLICATION. Collected papers from scientific and technical conferences, symposia, seminars, or other meetings sponsored or cosponsored by NASA.

- SPECIAL PUBLICATION. Scientific, technical, or historical information from NASA programs, projects, and missions, often concerned with subjects having substantial public interest.

- TECHNICAL TRANSLATION. English-language translations of foreign scientific and technical material pertinent to NASA's mission.

Specialized services also include creating custom thesauri, building customized databases, organizing and publishing research results.

For more information about the NASA STI program, see the following:

- Access the NASA STI program home page at *http://www.sti.nasa.gov*

- E-mail your question to *help@sti.nasa.gov*

- Fax your question to the NASA STI Information Desk at 443–757–5803

- Phone the NASA STI Information Desk at 443–757–5802

- Write to:
  STI Information Desk
  NASA Center for AeroSpace Information
  7115 Standard Drive
  Hanover, MD 21076–1320

NASA/TM—2013-216562 AIAA–2013–3727

Investigation of Insulation Materials for Future Radioisotope Power Systems

Peggy A. Cornell, Frances I. Hurwitz, and David L. Ellis
Glenn Research Center, Cleveland, Ohio

Paul C. Schmitz
Vantage Partners, LLC, Brook Park, Ohio

Prepared for the
11th International Energy Conversion Engineering Conference (IECEC)
sponsored by the American Institute of Aeronautics and Astronautics
San Jose, California, July 14–17, 2013

National Aeronautics and
Space Administration

Glenn Research Center
Cleveland, Ohio 44135

December 2013

Acknowledgments

This work is funded through the NASA Science Mission Directorate. The authors wish to acknowledge the people who made this effort possible including Katie Shaw and Justin Elchert for providing considerable analytical and modeling guidance; Haiquan Guo for her materials expertise and composite fabrication; Adrienne Veverka, Jesse Bierer, and Grant Feichter for their technical dedication to our experimental testing; Don Jaworske for enabling our emissivity testing; and Terry O'Malley, Lee Mason, and Duane Beach for supporting this effort under the Radioisotope Power Systems (RPS) program.

This report contains preliminary findings, subject to revision as analysis proceeds.

Level of Review: This material has been technically reviewed by technical management.

Available from

NASA Center for Aerospace Information
7115 Standard Drive
Hanover, MD 21076–1320

National Technical Information Service
5301 Shawnee Road
Alexandria, VA 22312

Available electronically at http://www.sti.nasa.gov

Investigation of Insulation Materials for Future Radioisotope Power Systems

Peggy A. Cornell, Frances I. Hurwitz, and David L. Ellis
National Aeronautics and Space Administration
Glenn Research Center
Cleveland, Ohio 44135

Paul C. Schmitz
Vantage Partners, LLC
Brook Park, Ohio 44142

Abstract

NASA's Radioisotope Power Systems (RPS) Technology Advancement Project is developing next-generation high-temperature insulation materials that directly benefit thermal management and improve performance of RPS for future science missions. Preliminary studies on the use of multilayer insulation (MLI) for Stirling convertors used on the Advanced Stirling Radioisotope Generator (ASRG) have shown the potential benefits of MLI for space vacuum applications in reducing generator size and increasing specific power (W/kg) as compared to the baseline Microtherm HT (Microtherm, Inc.) insulation. Further studies are currently being conducted at NASA Glenn Research Center on candidate MLI foils and aerogel composite spacers. This paper presents the method of testing of foils and spacers and experimental results to date.

Nomenclature

Al_2O_3	aluminum oxide (alumina)
ASC	Advanced Stirling Convertor
ASRG	Advanced Stirling Radioisotope Generator
atm	atmosphere
DAQ	data acquisition
Fe_2O_3	iron oxide
GPHS	General Purpose Heat Source
ID	inside diameter
MLI	multilayer insulation
MPS	Moulded Pipe Section
Na_2O_3	sodium oxide
OD	outside diameter
RPS	Radioisotope Power Systems
SiO_2	silicon dioxide (silica)
TEOS	tetraethyl orthosilicate
ZrO_2	zirconium dioxide (zirconia)

Introduction

The Advanced Stirling Radioisotope Generator (ASRG) is under development by the Department of Energy and Lockheed Martin Space Systems Company. It comprises two Advanced Stirling Convertors (ASCs), which are being developed by an integrated team of Sunpower, Inc., and the NASA Glenn Research Center. The ASC development, funded by NASA's Science Mission Directorate, started as a technology development effort in 2003 and has since evolved through progressive convertor builds and

successful testing to demonstrate high conversion efficiency, low mass, and capability to meet long-life Radioisotope Power Systems (RPS) requirements. The objective of the ASRG's insulation package is twofold: to minimize the loss of thermal energy from the Plutonium-238 General Purpose Heat Source (GPHS) to the environment and to act as a passive safety device in the event of single convertor stoppage. In the latter case, the insulation would permanently shrink to allow a sufficient heat leak, ensuring that the iridium cladding in the GPHS never exceeds its design temperature.

Preliminary studies have been done on the use of multilayer insulation (MLI) in the ASRG. These studies show the potential benefits of MLI for space vacuum applications in reducing generator size and increasing specific power (W/kg) as compared to the baseline Microtherm HT (Microtherm, Inc.) insulation. Thermal losses from the Microtherm HT insulation currently used in the ASRG are estimated to exceed 25 percent (62.3 W_{th} on the ground (1 atm Argon)) and 15 percent (37.8 W_{th}) in a vacuum of the total 244.0 W_{th} generated by the GPHS (Ref. 1). Studies show these losses can be reduced through the substitution of MLI for the Microtherm HT currently used in the ASRG. A schematic of the ASRG and its insulation package is shown in Figure 1.

The MLI consists of several layers of closely spaced, highly reflective shields, or foils, which are placed perpendicular to the heat flow direction. These low emissivity foils provide a thermal high resistance to radiative heat transfer between layers. To avoid direct contact between the foils, and therefore heat conduction between the sheets, low-conductivity and nonmetallic spacers are used. A sketch of a typical MLI is shown in Figure 2.

The theoretical thermal conductivity of MLI (using nickel foils and ZrO_2 spacers) has been found to be approximately two orders of magnitude less than that of fibrous bulk insulations at 1000 °C in a vacuum environment (Ref. 2). To help better quantify the characteristics and potentially increase the temperature range of state-of-the-art MLI, a development effort is underway to expand our experimental test rig capabilities; identify, test, and analyze candidate materials; and optimize data collection and thermal modeling at Glenn. This effort is key in that insulation materials directly benefit thermal management and could improve performance of RPS for future science missions.

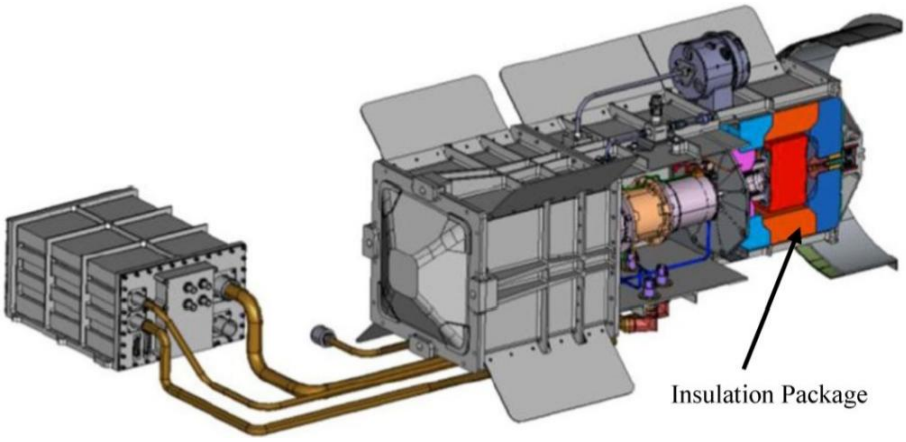

Figure 1.—Advanced Stirling Radioisotope Generator (ASRG) featuring insulation package.

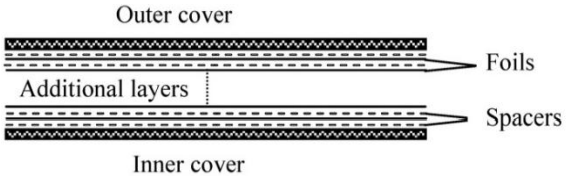

Figure 2.—Sketch of a typical multilayer insulation (MLI). Foils are denoted by a solid line and spacers by a dashed line.

Experimental Testing

Insulation Test Rig and Test Methodology

The design goal of the experimental test rig was to establish one-dimensional heat flow through an insulation sample to compare MLI candidates including foil/aerogel hybrid insulations for future RPS. A secondary goal was to configure the rig for relatively convenient interchangeability of the test samples and addition of instrumentation as needed. The MLI rig and test station can be seen in Figure 3.

The test rig consisted of a heat source and a vertical MLI stack surrounded by a Microtherm Moulded Pipe Section (MPS) holder. The heat source was a HeatWave Laboratory Model #102104 (HeatWave Labs, Inc.) heater enclosed in a custom housing. The inside diameter (ID) of the MPS holder was made to slip over the outside diameter (OD) of the custom heater housing and enclose the heater and MLI stack. The MPS holder insulated the MLI stack and the heater, minimizing heat loss in the radial direction, as well as optically enclosing the test sample. The MPS holder was made of a microporous silica insulation with a nominally 102 mm (4 in.) ID and 114 mm (4.5 in.) OD that was wrapped in E-Glass cloth for easy handling. Its rated thermal conductivity in air was 0.034 W/mK at a mean temperature of 800 °C, the highest temperature tested by the manufacturer (Ref. 3). The heater, which was made of tungsten, has a three-layer heat shield on the back side to minimize heat loss in the downward direction. Its heating elements were covered by a molybdenum plate that acted as a heat spreader. The heater was rated to operate at 1100 °C continuously in vacuum. Installation of the MPS holder around the tungsten heater is shown in Figure 4. The vertical MLI test sample stacks were constructed by alternating layers of metal foils and spacers. The spacers were ceramic fabric or paper with or without aerogel impregnation.

Figure 3.—Multilayer insulation (MLI) rig and test station.

Figure 4.—Moulded Pipe Section (MPS) holder installed around tungsten heater in multilayer insulation (MLI) rig. Image on left shows MPS holder being installed around the heater. Image on right shows MPS holder in its testing configuration.

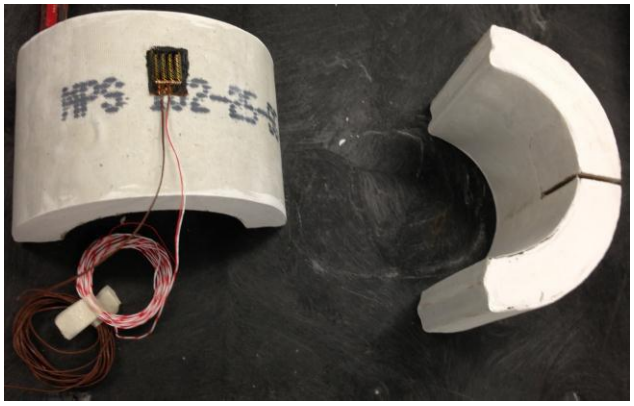

Figure 5.—Heat flux sensor installed on side of Microtherm MPS holder.

An RdF Model 27036–3 (RdF Corporation) heat flux sensor with integrated Type T thermocouple was adhered to the top foil in the MLI stack using OMEGABOND 200 (OMEGA Engineering, Inc.) high thermal conductivity two-part epoxy. The temperature and heat flux of the outside of the holder and backside of the heater were measured using RdF Models 27036–1 and 27036–3 heat flux sensors, respectively. The heat flux sensors were limited to a maximum temperature of 260 °C. The bottom heat flux sensor was consistently the hottest and therefore limited the maximum reference temperature of the test rig to approximately 625 °C. Figure 5 shows the heat flux sensor affixed to the outside of the MPS holder.

The entire assembly was mounted in a stainless steel bell jar. The bell jar was evacuated using a Leybold Model TMP 1000 C (Oerlikon Leybold Vacuum) turbopump to a pressure less than 8×10^{-6} torr to ensure that convection did not play a significant role in the heat transfer.

The top of the bell jar was water cooled to maintain a constant sink temperature of 20 °C. The uncooled sides of the bell jar that were outside of the view factor of the top foil heat up minimally during testing. The maximum temperature of these sidewalls was measured by a combination of reference thermocouples and infrared imaging of the exterior and found to be less than 35 °C at the maximum reference temperature.

An Ohio Semitronics PC8–002–01D (Ohio Semitronics, Inc.) direct current watt transducer and a variable frequency alternating current watt transducer measured the electrical power supplied to the heater and permitted a power balance calculation and determination of the potential heat losses through thermal shorts and other means not accounted for by the three heat flux sensors, for example, loss through the copper leads for the heater power and loss through the thermocouples.

The signals from the sensors were collected using up to four ICP DAS Model I–7011 (ICP DAS USA) data acquisition (DAQ) modules. The modules converted the analog signals to digital signals and sent the data over a local area network to the DAQ computer. A custom-written DAQ program was utilized to record data every 60 sec. This interval was sufficient to give adequate statistical data on the measurements.

During testing, the system was considered to be at steady state and test conditions at thermal equilibrium when the test environment pressure was less than 8×10^{-6} torr and the temperature of the top foil remained constant within 3 °C for 1 hr with no definite trend. The top foil thermocouple was used to determine thermal equilibrium since it was observed to be the last of the test environment thermocouples to reach thermal equilibrium. The thermocouple that defined reference temperature, or test rig temperature, during testing was located on the hottest (bottom) foil.

Candidate Materials

The ASC has an upper temperature limit of approximately 850 °C based on material life requirements. The ASCs in the ASRG currently operate below this maximum temperature due to improved overall power output (reduced heat losses through the insulation) at 760 °C. Using the ASC material limits of a nickel heat acceptor at 850 °C, the temperature of the inner surface of the insulation is typically 100 °C greater, or 950 °C. The candidate MLI foils and spacers must perform effectively within this temperature range. The foils and their respective material properties are listed in Table I.

TABLE I.—CANDIDATE FOILS FOR MLI TESTING

Metal	Melting point	Emissivity/temperature,[a] °C	Note	Measured emissivity/temperature, °C
Tantalum	3000 °C	0.14 to 0.30/727 to 2930	Unoxidized	0.0922/25
Nickel-niobium	1170 °C (eutectic)[2]	Ni = 0.05 to 0.19/38 to 1000 Nb = 0.12/1000	Unoxidized—only first layer Nb	Nickel = 0.0258/25 Niobium = 0.052/25
Molybdenum	2617 °C	0.06 to 0.18/38 to 1093	unoxidized	TBD
Gold	1063 °C	0.02 to 0.03/38 to 1093	Polished	TBD

[a]Per Table of Total Emissivity, www.omega.com .

Emissivity testing was performed at room temperature (25 °C) on the tantalum and nickel and niobium samples to verify their emissivity values, which can vary due to surface finish and oxidation. The measurements were obtained using an Infrared Reflectometer Model DB100 from Gier Dunkle Instruments, Inc. Reflectivity was measured and recorded at various locations on each sample, allowing to average the emissivity for each foil. The reflectometer was calibrated using a gold and black standard with reflectively values of 0.976 and 0.089, respectively. These measured emissivity values are also shown in Table I.

The candidate spacer materials under consideration, which have advanced insulating properties compared to zirconia spacers that have been used in the past, include APA–2 alumina paper (Zircar Ceramics, Inc.), Astroquartz silica fiber fabric (JPS Composite Materials), Fiberfrax 972AH alumina paper (Unifrax, LLC) and Saffil paper (Saffil, Ltd.). As shown in Figure 6, spectral properties of the candidate spacer materials are a primary factor in material selection for testing. Further consideration includes commercial availability and physical characteristics such as thickness and density. The physical and thermal characteristics, as well as composition, of the current candidate spacers are shown in Table II and their respective microstructures are shown in Figures 7 to 10.

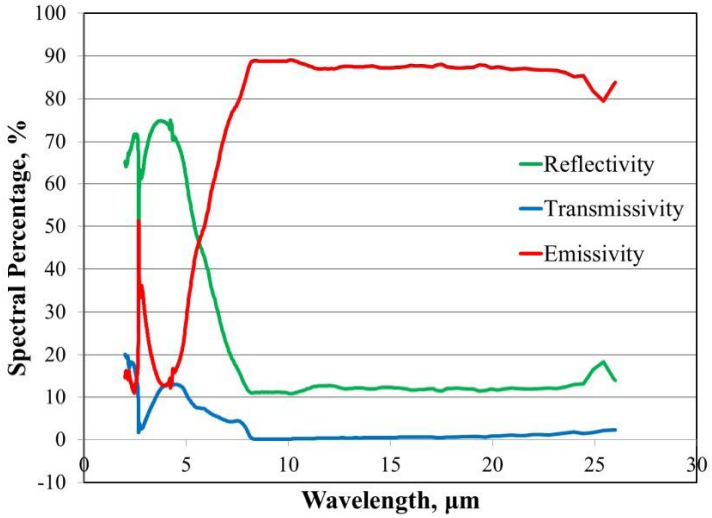

Figure 6.—Spectral properties of APA–2 paper with aerogel.

TABLE II. CANDIDATE SPACERS FOR MULTILAYER INSULATION (MLI) TESTING[a]

Ceramic reinforcement	Thickness, mm	Density, g/cc	Upper use temperature	Composition, percent
APA–2 paper	1.25	0.11	1650 °C	86 Al_2O_3, 10 SiO_2, and four other oxides
Fiberfrax 972AH	0.8	0.192	1176 °C	47-52 Al_2O_3, 48 to 53 SiO_2, <0.5 Na_2O_3, and <0.5 Fe_2O_3
Astroquartz (503 plain weave without binder)	0.11	2.2	1070 °C	99.99 SiO_2
Saffil paper	0.5 and 1.0	0.5 to 0.7	1600 °C	95 to 97 Al_2O_3, 3.0 to 5.0 SiO_2, and <0.5 trace elements

[a]As per manufacturer data.

Figure 7.—APA–2 microstructure.

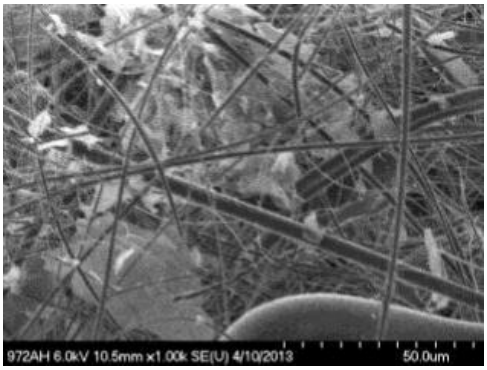

Figure 8.—Fiberfrax 972AH microstructure.

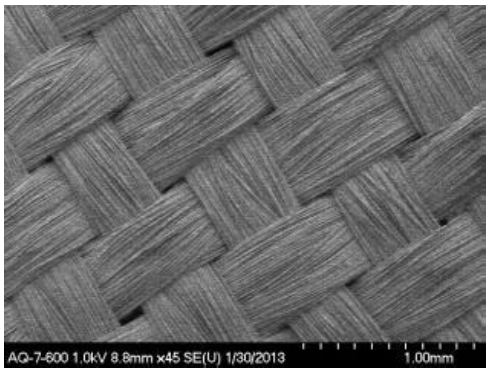

Figure 9.—Astroquartz fabric microstructure.

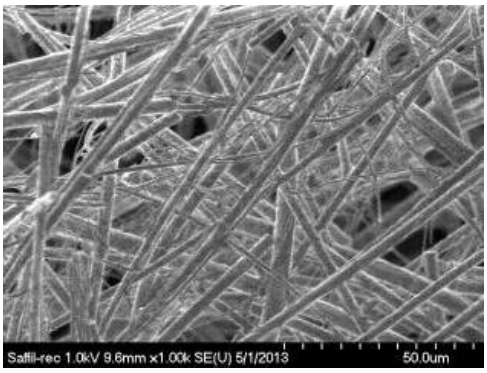

Figure 10.—Saffil paper microstructure.

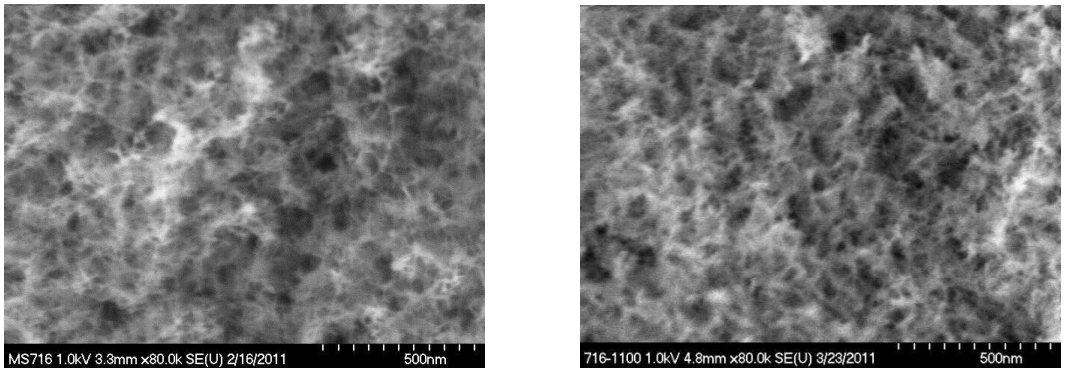

Figure 11.—Microstructure of the as-supercritically dried aluminosilicate aerogel before and after 20 min of exposure at 1100 °C. Image on left shows before drying (surface area is 415 m^2/g). Image on right shows after drying (surface area is 266 m^2/g).

Characterization of insulation materials has substantially progressed and material scientists at Glenn Research Center are presently studying aerogel materials with increased temperature capability and lower densities compared with state-of-the-art polymer-based insulating materials. Composites such as those currently under consideration impregnated with aerogel offer potential as spacers between MLI foils.

Aerogels are mesoporous structures with interconnecting pores and high surface areas; the pore walls comprise thin struts that provide a lengthy and tortuous path limiting solid conduction from foil to foil. In an application with any gaseous environment, gas convection is limited by the small-scale pore structure; in both atmosphere and vacuum, extinction of radiation heat transfer takes place by absorption (Ref. 4) and is wavelength and temperature dependent. The effective thermal conductivity also is expected to be influenced by the emissivity of the adjacent foils (Ref. 5).

Although numerous studies have been conducted on silica aerogels, aerogels can be synthesized using a wide variety of elements, and their upper use temperature is limited by their chemical composition. Hence, polymeric aerogels are limited by the decomposition temperature of the particular polymer (> 400 °C for some polyimides). Silica aerogels sinter above 700 °C, losing their high surface area and becoming less insulating. NASA Glenn Research Center has developed aluminosilicate aerogels that maintain high surface areas and mesoporous structures to temperatures of 1100 to 1200 °C. They are produced through the reaction of boehmite and tetraethyl orthosilicate (TEOS), in which the surface area and pore structure can be controlled by the choice of boehmite precursor and the synthesis parameters (Refs. 6 and 7). The aluminosilicate aerogels in the present study utilize an aluminum to silicon ratio of 3 to 1, the ratio found in mullite.

Microstructures of the as-supercritically dried aerogel, and the same aerogel after 20 min of exposure at 1100 °C, are shown in Figure 11. The surface area decreases from 415 to 266 m^2/g on exposure, and the pore volume decreases from 0.67 to 0.44 cm^3/g. A mesoporous structure is maintained, with the average pore diameter changing from 7.44 to 8.15 nm.

Because of the fragile nature of the aluminosilicate aerogel monoliths, Glenn has developed techniques for incorporating them into composites, which can be reinforced using ceramic fabrics, papers, or felts. The work presented here focuses on the use of APA–2 alumina paper. Composites also have been fabricated using Astroquartz silica fiber fabric and Fiberfrax 972AH alumina paper. The composites remain flexible (Fig. 12), which would be advantageous in forming an MLI around the GPHS. The APA–2 composite has a density of 0.15 g/cm^3, as compared with 0.3428 g/cm^3 for Microtherm HT. The aluminosilicate aerogel bonds well to the alumina fibers (Fig. 13), averting the spalling of aerogel particles seen in some commercial materials.

Figure 12.—Aerogel composite reinforced with APA–2 alumina paper.

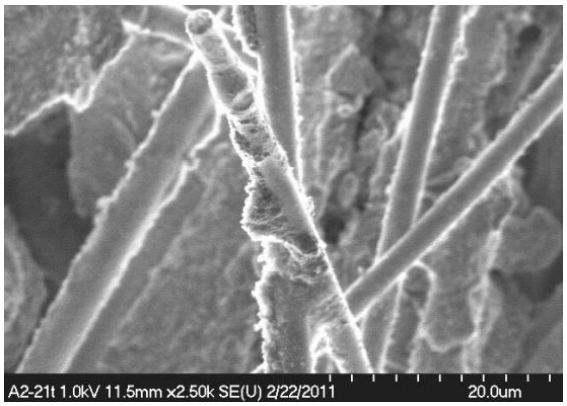

Figure 13.—Microstructure of APA–2 with aerogel composite showing good wetting of aerogel to fibers.

Modeling

A Thermal Desktop (Cullimore & Ring Technologies, Inc.) model of the insulation sample and surrounding environment was created to estimate the thermal performance of the test foils (Fig. 14). The model included the following test rig components: foils with temperature dependent properties, spacers, heat source, and test chamber (approximated as a single isothermal boundary).

Currently, poor correlation exists between the test results and the model, therefore, modification of both the test rig and the model are underway. Heat losses, such as edge effects (radiation from the edges of the MLI stack), were present primarily due to the small test sample size of 102 mm (4 in.) in diameter.

Several heat transfer paths and mechanisms can strongly influence the model predictions and associated uncertainty and error propagation. One testing attribute being investigated is to experimentally determine the effect of spacer thickness on MLI performance. Thick or multiple spacer layers allow for the placement of thermocouples between foil layers with minimum physical perturbation of the foils. Test runs are also underway with thermocouples at only the hot and cold sides of the stack as well as each layer of the stack to evaluate the influence of radial heat transfer along the thermocouple leads. Once the heat transfer paths are identified, the MLI test rig will be redesigned in an attempt to mitigate heat leaks, improve data fidelity, and reduce associated error. An exploded view of the current test setup, generated through modeling tools, is shown in Figure 15 with respective callouts in Table III.

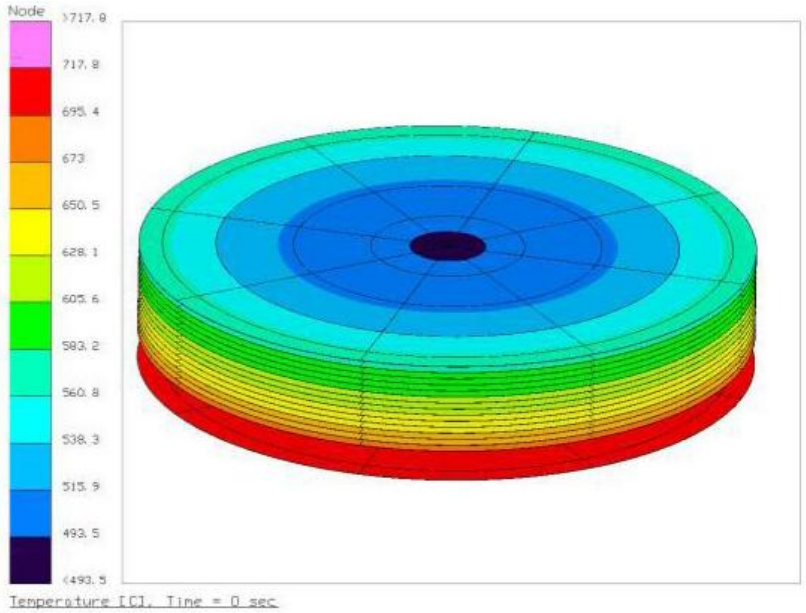

Figure 14.—Multilayer insulation (MLI) model results using Thermal Desktop.

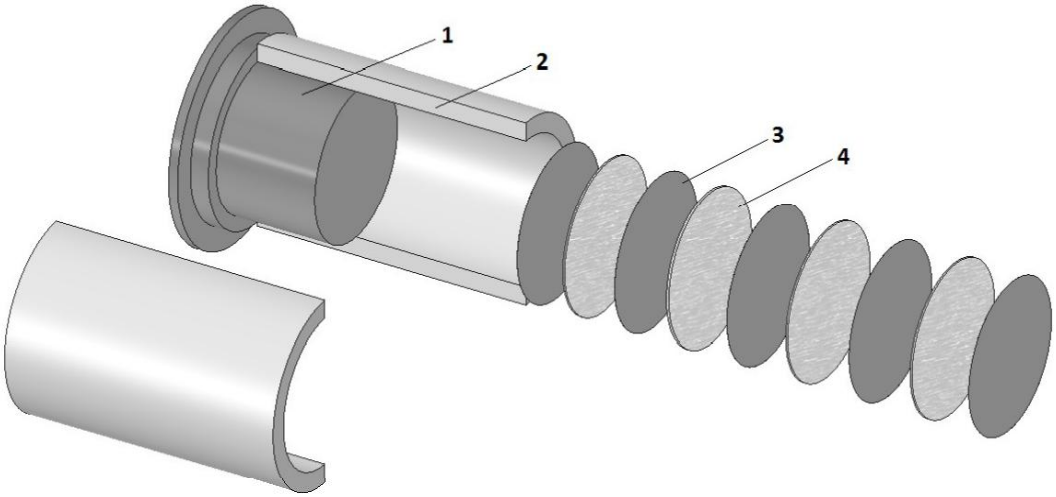

Figure 15.—Exploded view of the primary test section components and multilayer insulation (MLI) test sample.

TABLE III.—LOCATIONS OF THE PRIMARY TEST SECTION COMPONENTS AND MULTILAYER INSULATION (MLI) TEST SAMPLE AS SHOWN IN FIGURE 15

Callout	Description
1	Heater assembly
2	Moulded Pipe Section (MPS) holder
3	Foil
4	Spacer

Experimental Results

Tantalum Foils With APA–2 Alumina Paper

The first MLI run consisted of tantalum foils and APA–2 alumina paper spacers. The thickness of the MLI stack was approximately 13 mm (0.5 in.). The temperature within the MLI test rig was increased as shown in Figure 16 and held until the system was considered to be at steady state and test conditions at thermal equilibrium (pressure was less than 8×10^{-6} torr and temperature of the top foil remained constant within 3 °C for 1 hr with no definite trend).

As seen in Figure 16, the maximum operating temperature that was reached with this foil and spacer combination was approximately 600 °C. This was because the heat flux sensors that were utilized were limited to a maximum operating temperature of 260 °C. The bottom heat flux sensor, located on the heat shield of the heater, was consistently the hottest and therefore limited the maximum reference temperature of the rig. In this test, a maximum of 600 °C was reached, as shown in Figure 16.

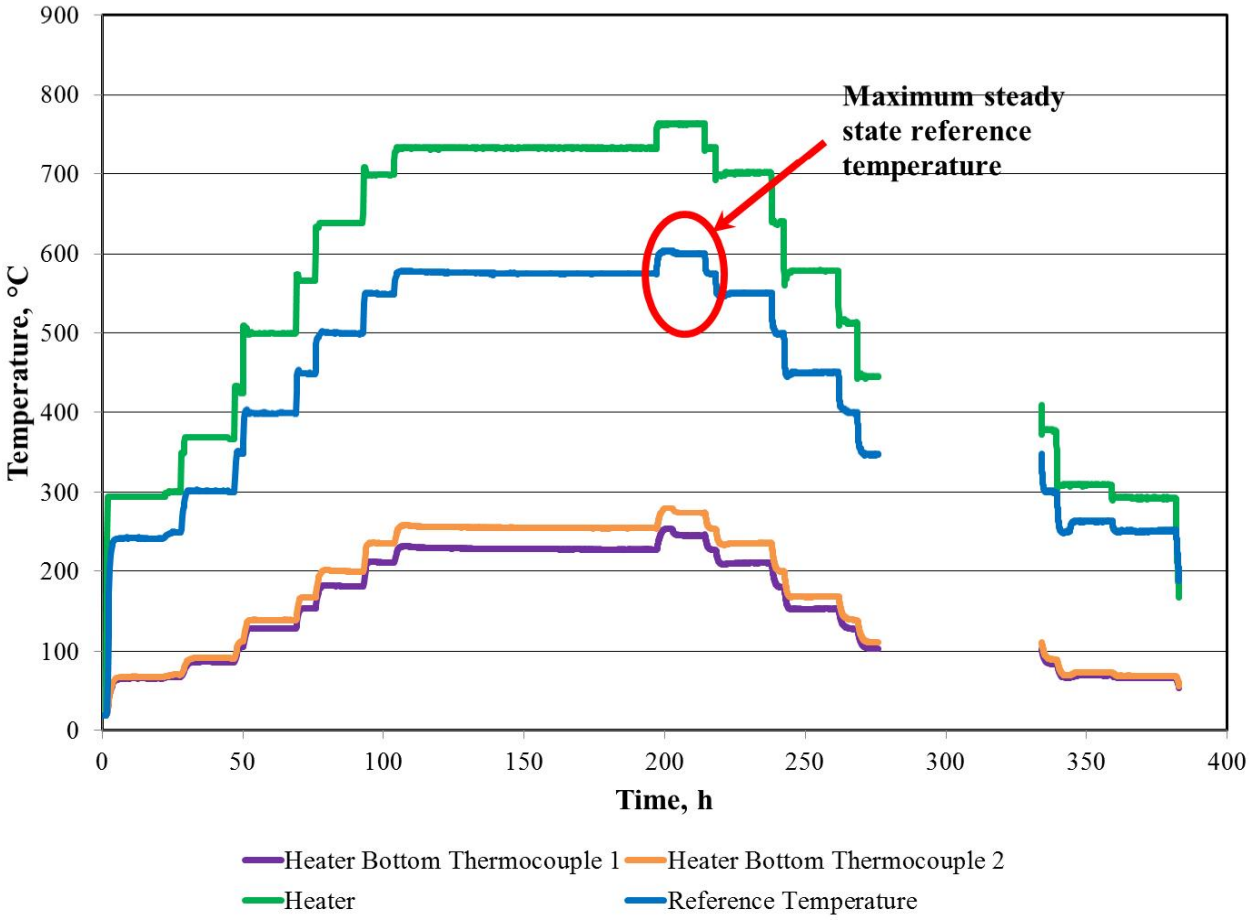

Figure 16.—A typical time versus temperature plot for the tantalum foils with APA–2 alumina paper. The data at maximum test rig temperature are circled. Loss of signal occurred between approximately 273 and 325 hr.

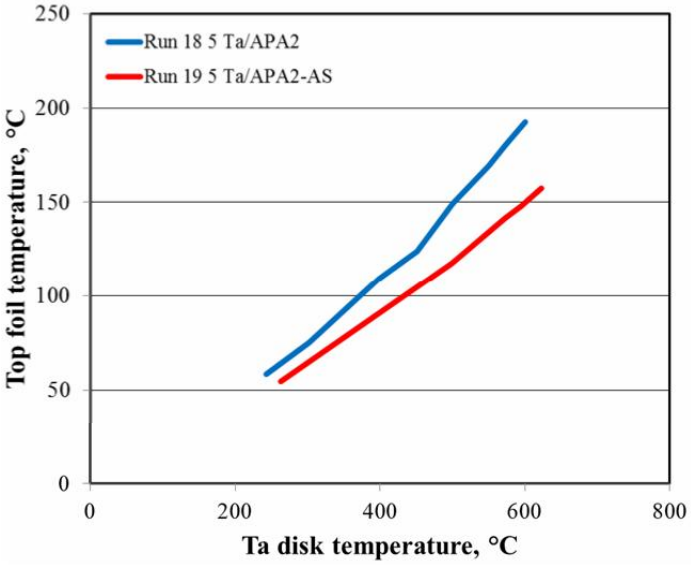

Figure 17.—Comparison of tantalum foils with APA–2 paper and tantalum foils with APA–2 paper with aerogel. The blue plot represents the tantalum/APA–2 temperatures and the red plot represents the tantalum/APA–2 with aerogel temperatures. The x-axis displays reference temperatures and the y-axis displays the coldest foil temperature (top of multilayer insulation (MLI) stack).

Tantalum Foils With APA–2 Alumina Paper Impregnated With Aluminosilicate Aerogel

The subsequent test run consisted of tantalum foils and APA–2 alumina paper spacers impregnated with aluminosilicate aerogel. The test rig conditions remained the same as the previous test, and the maximum temperature reached was approximately 625 °C. Test results of the tantalum foils with and without aerogel-impregnated spacers were similar. The exception was that the temperature of the top (coldest) tantalum foil within the stack was approximately 40 °C less at a test rig temperature of 600 °C for the aerogel-impregnated spacers (Fig. 17). The data captured in Glenn's MLI test rig indicated that the composite spacer with aluminosilicate aerogel reduced heat transfer compared to the composite spacer without aerogel. Further testing and analysis is required to confirm repeatability of these preliminary results and to determine the basis for the temperature difference.

Conclusion

Insulation materials have a significant effect on decreasing the thermal losses and increasing specific power (W/kg) of Radioisotope Power Systems (RPS). To help better quantify the characteristics and potentially increase the temperature range of state-of-the-art multilayer insulation (MLI), a development effort is underway to expand our experimental test rig capabilities; identify, test and analyze candidate materials; and optimize data collection and thermal modeling at NASA Glenn Research Center. Heat flow through insulation samples was achieved in the newly developed MLI test rig and thermal measurement methods and predictions are progressing. Characterization of insulation materials has substantially advanced and aerogel materials with increased operating temperature and decreased density are being studied for use as composite spacers in MLI. Future testing will consider foil/spacer combinations that are suitable in high temperatures, can remain flexible to form an effective MLI around the General Purpose Heat Source (GPHS) of the Advanced Stirling Radioisotope Generator (ASRG), and are thin and low in density to potentially reduce generator size and increase specific power as compared to the baseline Microtherm HT insulation.

References

1. Wang, X.J.; Fabanich, W.A.; and Schmitz, P.C.: Advanced Stirling Radioisotope Generator Thermal Power Model in Thermal Desktop SINDA/FLUENT Analyzer. AIAA 2012–4060, 2012.
2. Thermo Electron Corp: Application of Multi-Foil Insulation to the Brayton Isotope Power System and Conceptual Design of Multi-Foil Insulation for the Flight System (Phase I). U.S. Department of Commerce Preliminary Design Review Document TE420910076, June 1976.
3. Promat High Performance Insulation Microtherm® MPS Moulded Pipe Section brochure from http://www.microthermgroup.com/landingpage/assets/TDS_MICROTHERM_MPS_V1-EN.pdf.
4. Heinemann, U., et al.: Radiation-Conduction Interaction: An Investigation on Silica Aerogels. Int. J. Heat Mass Transfer, vol. 39, no. 10, 1996, pp. 2115–2130.
5. Scheuerpflug, P., et al.: Apparent Thermal Conductivity of Evacuated SiO_2-Aerogel Tiles Under Variation of Radiative Boundary Conditions. Int. J. Heat Mass Transfer, vol. 28, no. 12, 1985, pp. 2299–2306.
6. Hurwitz, F.I., et al.: Tailoring of Boehmite-Derived Aluminosilicate Aerogel Structure and Properties: Influence of Ti Addition. Materials Research Society Fall Meeting, Boston, MA, 2010.
7. Hurwitz, F.I., et al.: Influence of Ti Addition on Boehmite-Derived Aluminum Silicate Aerogels: Structure and Properties. J. Sol-Gel Sci. Technol., vol. 64, no. 3, 2012, pp. 756–764.